Depth Distribution Functions of Secondary Electron Production and Emission

Z.J. Ding*, Y.G. Li, R.G. Zeng, S.F. Mao, P. Zhang and Z.M. Zhang
Hefei National Laboratory for Physical Sciences at Microscale and Department of Physics, University of Science and Technology of China, Hefei, Anhui 230026, P.R. China
*zjding@ustc.edu.cn

(Received: Jan. 31, 2009; Accepted: February 17, 2009)

As fundamental importance to SEM observation of specimen surface, secondary electron generation and emission processes have been studied by a Monte Carlo method. The simulation is based on a discrete description of cascade secondary electron production. The Monte Carlo model combines the use of Mott's cross section for electron elastic scattering and of Penn's dielectric function for electron inelastic scattering. Two models of dielectric function, i.e. the single pole approximation and the full Penn algorithm, are shown to give energy distribution and yield of secondary electrons in agreement with experimental results for non-free electron materials and free electron metals, respectively. We use a constructive solid geometry modeling to describe sample 3D geometry and a Gaussian function to describe random surface roughness. The technique is efficient and powerful in a simulation of SEM images of secondary electrons and backscattered electrons for a quite complex geometry of nanostructures. Finally we present the depth distribution functions for secondary electron generation and emission. Their dependences on primary energy and atomic numbers are analyzed. Furthermore, we shall also discuss a general issue of depth distribution function for rough surfaces.

1. Introduction

Scanning electron microscope (SEM) imaging of surface micro-structures by using secondary electrons and backscattered electrons, escaped from the specimen surface under a primary electron beam bombardment, as image signals has been played as an basic tool for the study of various kinds of materials in many scientific and technological fields. Secondary electron images, formed by secondary electrons of very low energies (several eV) that emitted from the surface region, provide mainly the topographic information of specimen surface with a resolution up to subnanometer for a modern SEM. Understanding of the related secondary electron emission phenomenon is thus essential to analyze SEM imaging contrast formation and also for a theoretical understanding of electron-solid interaction process [1]. A lot of works including both experimental and theoretical investigations have already been done on the secondary electron emission phenomena. This paper summarizes from several respects the recent developments on our study secondary electrons by a Monte Carlo simulation method.

2. Monte Carlo Model

We have proposed a physical model for the simulation of secondary electron generation [2,3]. In short the model is based on the use of Mott cross section in describing electron elastic scattering and a dielectric function approach to electron inelastic scattering. Individual electron scattering events are thus simulated by random sampling of physical quantities, such as, step length, scattering angle, loss energy etc, from respective cross sections. Each individual inelastic collision may produce a knock-on secondary electron by transferring loss energy to an inner-shell electron or a valence electron. Secondary electron transport in a solid follows the similar scattering processes as the primary electron, resulting in a cascade process of secondary electron production.

For the modeling of electron inelastic scattering Penn [4] has developed an algorithm to derive the basic quantity, i.e. the energy loss function, by using optical data for a theoretical evaluation of electron inelastic scattering free path (IMFP) based on dielectric function theory; but the implementation of this algorithm in the calculation of IMFP and stopping power up to now has been totally done by using the so-called single pole approximation (SPA). But, SPA becomes inaccurate when the energy decreases down to the plasmon excitation energy; therefore, it is not applicable to a Monte Carlo simulation of secondary electrons, at least, for free-electron-like materials. We have then proposed [5] to employ the full Penn algorithm (FPA) to the calculation of the differential IMFP. Furthermore, a consistent scheme of calculation is necessary for the excitation of secondary electrons with the full Penn

Copyright (c) 2009 by The Surface Analysis Society of Japan

algorithm. The effectiveness of this new model for the simulation of cascade electron generation can be confirmed by comparing the simulated energy spectra and the yields of secondary electrons with the experimental data.

3. Sample Geometry Modelling

We have extended the simulation from a simple bulk sample with smooth surface to an inhomogeneous specimen with surface roughness. A complex sample geometry in nano scale would be an important studying subject for future SEM metrology. For such a simulation of materials made of complex geometric structures having different atomic compositions in each spatial zone, one has to specify the shape of the structure. Two chief available methods to construct the structure are the constructive solid geometry (CSG) modeling and the surface representation modeling.

The CSG modeling enables a complex sample geometric structure which is complex in elemental distribution as well as in topographical configuration being constructed with some simple 3D objects such as, sphere, cube and etc., which can be analytically described with finite number of parameters. The basic objects can be either vacancy or filled with elements, alloys or compounds. For an inhomogeneous specimen the conventional sampling procedure of the step length is unsuitable because the electron scattering mean free path or the scattering cross section is now position-dependent. Correction must be made in order to track the precise electron scattering trajectories in an inhomogeneous specimen. This correction to the step length is important for specimen containing nano scale structures so that the electron scattering mean free path is comparable with or even larger than the structure feature size. We use a ray-tracing technique in the calculation procedure of electron steps that across the different element zones.

For representation of surface roughness we employ a method in computer graphics by using finite element triangulated mesh to describe the sample surface. The surface roughness can be parameterized by the amplitude and the density of rough peaks. A Gaussian function is used here to model the rough effects. Therefore, we represent the random surface roughness by introducing two parameters: the 3σ deviation of a Gaussian function describes the amplitude fluctuation of rough peaks, and, the mesh interval describes the density of rough peaks. By varying the two parameters we can obtain a variety of rough surfaces or rough edges. The reason to use a triangulated mesh is due to its advantage on easy judging the intersection of a velocity vector with a local triangulated plane when considering an electron incidence into the surface or emission from the surface. Fig. 1 is an example of mesh building of a rough line, where each surface is roughness modulated. For a Monte Carlo simulation we have also to combine a block dividing technique with the description of the sample surface of 3D objects for accelerating the calculation. This technique can improve significantly the calculation efficiency for a quite complex geometry.

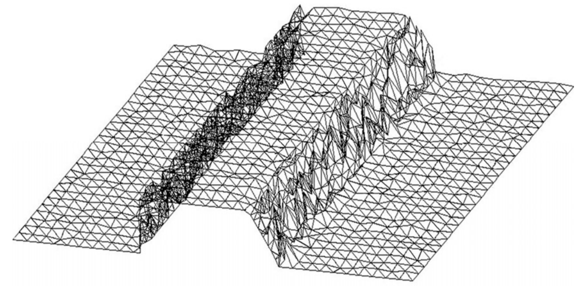

Fig. 1 Example rough surface structure modelling of a trapezoidal line.

4. Energy Distribution and Yield

Calculation of energy distribution and yield of secondary electrons must be firstly carried out before discussion of depth distribution functions in order to verify a Monte Carlo simulation model. Previous studies [3,5,9,10] have shown that the present Monte Carlo model can indeed describe very reasonably the experimental results. After further improving the evaluation of barrier potential for electron emission, the Monte Carlo simulated energy distribution of secondary electrons agree with experiment very well (Fig.2). Furthermore, FPA can produce reasonable energy distribution for free-electron-like metals while SPA could not.

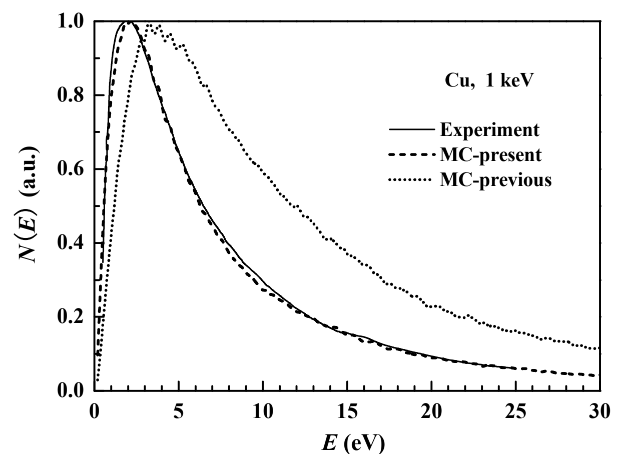

Fig. 2 Comparison on the energy distribution between an experiment and the Monte Carlo simulation results with SPA (the present result is obtained after barrier correction and for a rough surface: $\sigma = 3$ nm, $a = 5$ nm).

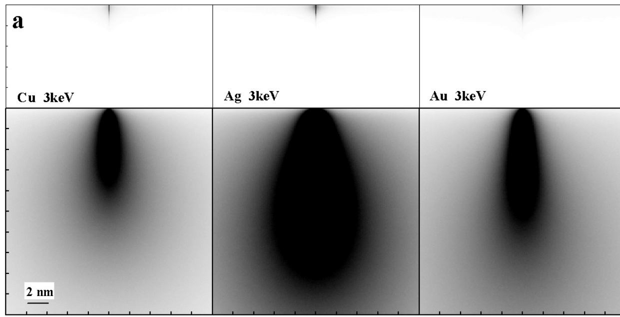

Fig. 3 Monte Carlo simulated spatial distributions of cascade secondary electron production (lower) and emission (upper) for several elements.

5. Depth Distribution Functions

Fig. 3 demonstrates the simulation results of spatial distribution of cascade secondary electron production and emission inside a solid for a point electron beam incidence. It clearly shows that, in addition to the importance of the lateral profile of secondary electrons to resolution of a SEM, the depth distribution is important to analyze the signal formation under the surface. Only those secondary electrons produced within the range several nanometers beneath a surface can be emitted to become signals. The range obviously depends on chemical composition of the material and the primary energy.

Then, two depth distribution functions may be defined in a way analogous to that in Auger electron spectroscopy (AES) [11,12]. One is the excitation depth distribution function (EXDDF), Φ , and another one is the emission depth distribution function (EMDDF), ϕ. However, here secondary electrons have no a unique characteristic energy because true secondary electrons are defined within a large energy range, 0-50 eV above vacuum level. The cascade production property of secondary electrons implies that the secondary electrons are still remained as signals by any energy decay in an inelastic scattering. Therefore, both EXDDF and EMDDF are considered as energy E dependent, where E is the excited energy. After the emission from the surface the energy of secondary electrons may change. Another distribution ψ may be defined according to the measured energy E_m of emitted true secondary electrons. Both integrals of ψ and the production of EXDDF and EMDDF give directly the secondary electron yield:

$$\delta = \int dE_m dz\, \psi(E_m, z) = \int dE dz \left[\Phi(E,z)\cdot\phi(E,z)\right].$$

The EXDDF may be defined with the excitation function as:

$$\Phi = n\int_{4\pi}\int_{E}^{E_p} I(E',z,\theta)\cdot\sigma_E(E')\left|\sec\theta\right| dE'\, d\Omega_\theta$$

where E' is energy of inelastic scattering electron

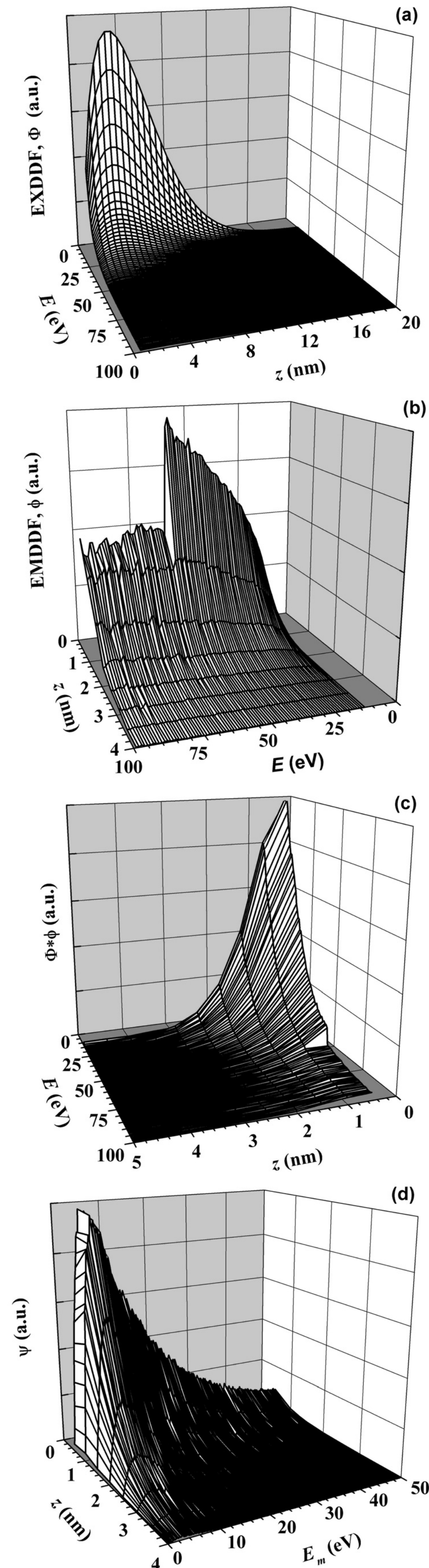

Fig. 4 Monte Carlo simulated results of (a) EXDDF; (b) EMDDF; (c) EXDDF*EMDDF; (d) depth distribution ψ for emitted secondary electron signals, for Cu at 1 keV.

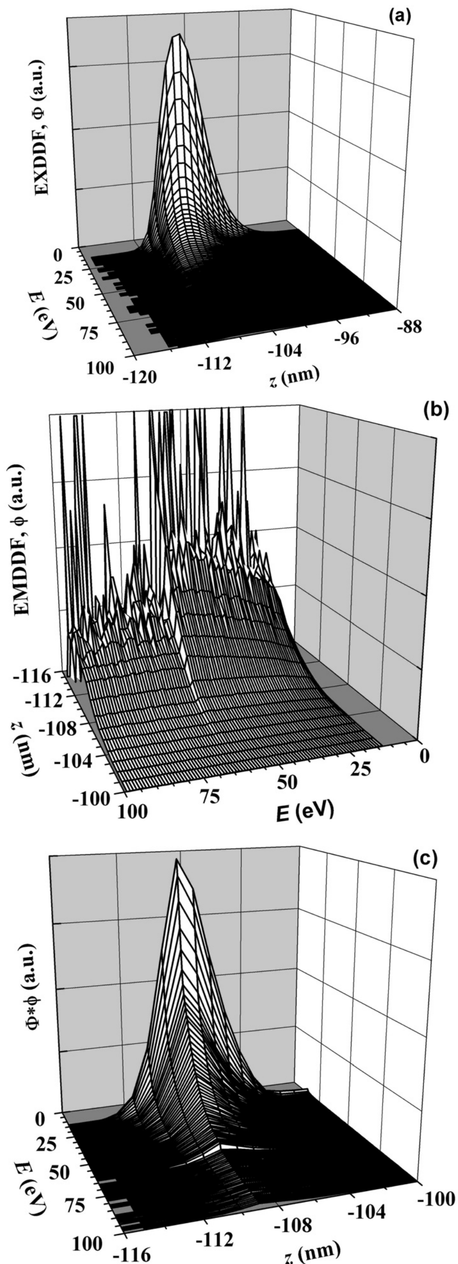

Fig. 5 Monte Carlo simulated results of (a) EXDDF; (b) EMDDF; (c) EXDDF*EMDDF, for Cu at 1 keV. The surface is described by a random roughness ($\sigma = 3$ nm, $a = 5$ nm).

for secondary electron excitation. But it should be noted that cascade production process complexes the expression of electron intensity distribution. For EMDDF, it's depth dependence may be described by an exponential decay law as:

$$\phi = \phi_0 \exp\left[-\alpha\left(E\right)z\right]$$

where α is the absorption coefficient.

Figs. 4 and 5 show respectively the calculated depth distribution functions for smooth surface and rough surface. Their dependence on beam condition and sample property can be analyzed in detail. It can be seen that EMDDF is quite different from ψ. While for Auger electron signals in AES there is no such difference on the emission depth distribution between at the excitation and after emission. We will also discuss the absorption coefficient.

6. SEM Image

The calculation of emission intensity of secondary electrons and backscattered electrons by primary electrons bombarding the sample surface at different locations has lead to obtain the secondary electron and backscattered electron images. Fig. 6 demonstrates the simulated secondary electron images for a structured specimen at nano-scale.

For practical application to critical dimension (CD) metrology of nanostructures in the IC industry the CD-SEM images of gate lines with rough surfaces are calculated (Fig. 7). The results are compared very well with an experiment [7].

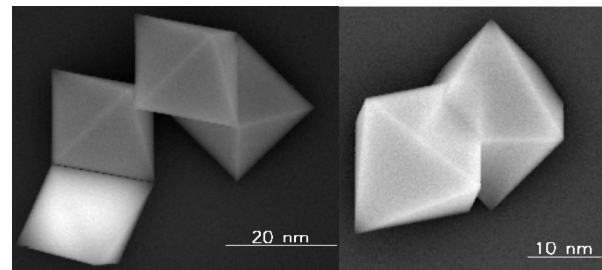

Fig. 6 Calculated SEM images of a complex structured sample.

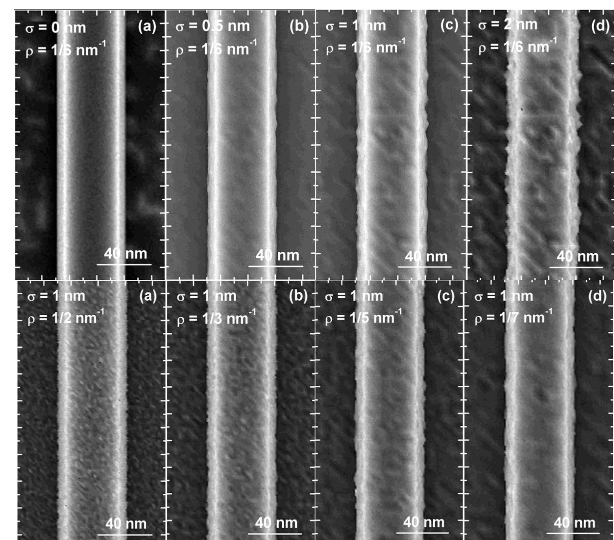

Fig. 7 Calculated SEM images of a rough trapezoidal Si line by modulating roughness amplitude and density.

7. Acknowledgement

This work was supported by the National Natural Science Foundation of China (Grant No. 10874160), '111' Project, Chinese Education Ministry and Chinese Academy of Sciences.

8. References

[1] R. Shimizu and Z. J. Ding, Rep. Prog. Phys. **55**, 487 (1992).

[2] Z. J. Ding and R. Shimizu, Scanning **18**, 92 (1996).

[3] Z. J. Ding, X. D. Tang and R. Shimizu, J. Appl. Phys. **89**, 718 (2001).

[4] D. R. Penn, Phys. Rev. B **35**, 482 (1987).

[5] S. F. Mao, Y. G. Li, R. G. Zeng and Z. J. Ding, J. Appl. Phys. **104**, 114907 (2008).

[6] H. M. Li and Z. J. Ding, Scanning **27**, 254 (2005).

[7] Y. G. Li, S. F. Mao, H. M. Li, S. M. Xiao and Z. J. Ding, J. Appl. Phys. **104**, 064901 (2008).

[8] Z. J. Ding, H. M. Li, K. Goto and R. Shimizu, J. Surf. Anal. **15**, 186 (2008).

[9] Z. J. Ding, H. M. Li, X. D. Tang and R. Shimizu, Appl. Phys. A **78**, 585 (2004).

[10] Z. J. Ding, H. M. Li, K. Goto, Y. Z. Jiang and R. Shimizu, J. Appl. Phys. **96**, 4598 (2004).

[11] A. Jablonski, Surf. Sci. **499**, 219 (2002).

[12] Z. J. Ding, W. S. Tan and Y. G. Li, J. Appl. Phys. **99**, 084903 (2006).